Multi-Area DC-OPF for HVAC and HVDC Grids

Emil Iggland, *Member, IEEE*, Roger Wiget, *Student Member, IEEE*, Spyridon Chatzivasileiadis, *Member, IEEE*, and Göran Anderson, *Fellow, IEEE*

***Abstract*—In interconnected power systems, operated by several system operators, the participating areas are strongly dependent on their neighbors. In order to identify the economically efficient generation dispatch in each area, a distributed multi-area optimal power flow (OPF) must be solved. Additionally, installation of an increasing number of HVDC lines to deal with increased power flows from renewable generation is expected to change the power system operation paradigm. The controllability introduced by the HVDC lines should be considered and incorporated in the OPF algorithm. In this paper we introduce a formulation for the distributed solution of the OPF problem in multi-area systems consisting of both HVAC and HVDC lines. We show the applicability of this formulation on two different operating schemes for HVDC grids and we compare their performance with a central solution for the mixed HVAC/HVDC grid. The proposed formulations are based on a linearized solution of the OPF problem. The only data to be exchanged between the areas pertains to the border nodes.**

***Index Terms*—DC power transmission, distributed algorithms, multi-area power systems, optimal power flow, power systems.**

I. Introduction

THE developments in the electric power systems in the last two decades have led to increased demand for long distance bulk power transmission [1], with an high voltage direct current (HVDC) super-grid being a possible solution [2]. This trend is compounded when considering the inclusion of large-scale renewable generation. HVDC lines are attractive options as they incur less losses over long distances, while they enhance the controllability of the power grid. The focus in this paper is on HVDC lines based on voltage source converter (VSC) technology (VSC-HVDC), which allow the formation of HVDC grids. Depending on the manner in which this grid is built different operating schemes will be required. Some of these operating schemes would need the coordination of multiple independent parties. The coordination has to consider the needs of the parties, as well as the different technologies used, primarily high voltage alternating current (HVAC) and HVDC.[1] In this paper, we introduce algorithms to provide this coordination between the independent parties and consider the integrated operation of both HVAC and HVDC grids.

A. Contributions of This Paper

The main new contribution of this paper is a multi-area optimal power flow (OPF) algorithm which, besides HVAC grids, incorporates the operation of HVDC grids. While a possible solution for a solution of HVAC-HVDC grids is presented in [3] and [4], in this paper a distributed optimization algorithm based on a linearized OPF formulation is proposed. Further, this paper describes three possible operating schemes for operating a multi-area HVDC grid. We present OPF formulations for all three operating schemes. The first formulation is a centralized solution to the case of mixed HVAC-HVDC grids, based on the work in [5], while the other two are distributed solutions. The linearized formulation that we propose can be used to account for interconnections independent of the technology used. An additional contribution of this paper is that compared to previous multi-area OPF formulations the one presented in this paper requires less variables to be exchanged, thereby reducing the amount of data which has to be exchanged per iteration. Further improvements are the removal of the need for a single system-wide reference bus, instead replacing it with a local reference bus in each area.

Besides the introduction of the distributed OPF formulations and the operating schemes, a case-study showing the properties of the distributed approach is also presented in this paper.

Although the formulation presented here can also be used to determine the security constrained optimal power flow (SCOPF) in a distributed manner, we will not consider the SCOPF problem in this paper. VSC-HVDC lines can react sufficiently fast and change their power flow after a contingency in order to maintain steady-state security, as already shown in [6]. Future work will extend the work presented in this paper, as well as in [7] and [8], to consider multi-area SCOPF formulations incorporating HVDC grids and corrective control capabilities of HVDC lines. The authors argue that the inclusion of security considerations in mixed HVAC-HVDC grids must take into account the controllable nature of the HVDC portion. Initial ideas for a possible solution of this problem is presented in [9] where a remedial action scheme is considered, as well as in [10], where a droop-controller is employed for the HVDC terminals. Reference [11] considers the effect of terminal outages in a pure HVDC grid.

B. Organization of This Paper

The paper is organized as follows: In Section II the proposed operating schemes are presented. In Section III the employed system modeling is described. In Section IV the approach which is used to perform the calculations in a distributed manner is explained. In Section V a case study on the basis of a IEEE RTS96 three-area test system with an additional HVDC grid is shown. Section VI concludes the paper with a discussion and outlook. A list of variables is attached in Table VIII in the Appendix.

We denote as distributed a method where there is partial exchange of data between participants, who, in turn, solve a local optimization problem using this information. This is opposed to the decentral method where there is no exchange of data, and only the local properties are considered. Therefore, within the

Manuscript received February 02, 2014; revised June 04, 2014 and September 12, 2014; accepted October 17, 2014. Date of publication November 20, 2014; date of current version July 17, 2015. Paper no. TPWRS-00154-2014.

The authors are with the Power System Laboratory, ETH Zürich, Zürich, Switzerland (e-mail: iggland@eeh.ee.ethz.ch; wiget@eeh.ee.ethz.ch; schatzivasileiadis@lbl.gov; andersson@eeh.ee.ethz.ch).

Digital Object Identifier 10.1109/TPWRS.2014.2365724

[1]For the remainder of this paper, by mentioning HVDC lines we will always refer to VSC-HVDC lines.

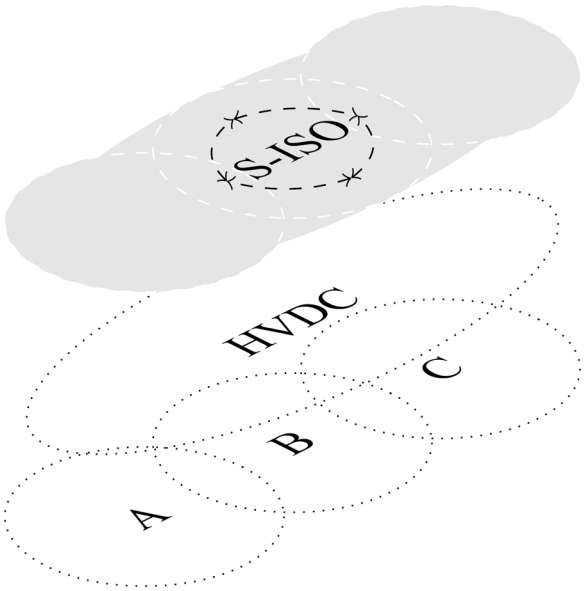

Fig. 1. Schematic depiction of operating scheme 1—"the Super ISO".

context of this paper, we will always refer to distributed, and not decentral, formulations of the OPF algorithm.

II. Operating Schemes

Under the current operating paradigm each independent system operator (ISO) is responsible for the operation of the grid which falls within their area of responsibility. With the introduction of an overlay HVDC grid this view of operation may be reconsidered.

The situation underlying this formulation is that there exist multiple ISOs who are connected to each other. As such the physical interconnection is modeled on the basis of the physical lines, and the generation capacity reflects that physically available. The limitations introduced are those given by the physical limitations of the lines.

We propose three operating schemes under which mixed HVAC-HVDC grids could be operated. The three operating schemes are depicted in Figs. 1–3. The first proposal is the centralization of all operations, leading to the operation of the grid by a single entity with complete knowledge and control. This proposal will be called operating scheme 1. The second proposal is the creation of a new ISO for the HVDC portion of the grid. This proposal will be called operating scheme 2. This new ISO has no knowledge of the HVAC portion of the grid, but complete knowledge of the HVDC grid. The traditional split of the HVAC ISOs is maintained along their borders. The third proposal is an extension of the current operation to include the HVDC grid portion of each ISO area. This proposal will be called operating scheme 3. Table I shows an overview of the differences between these schemes. The creation of a central ISO may create substantial regulatory and political issues arising from the fact that the participating ISOs would have to give up their power, responsibility and control to the central entity. The creation of an HVDC grid ISO is reasonable from the perspective that this grid may be built as the result of the inter-connection of a number of point-to-point HVDC links. In this situation it is likely that the previous owners and operators will coordinate their interconnection with the creation

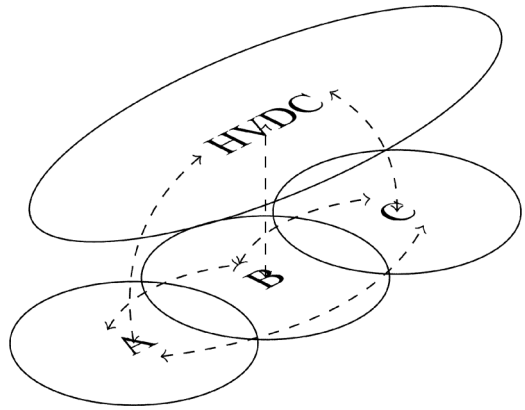

Fig. 2. Schematic depiction of operating scheme 2—"the HVDC ISO".

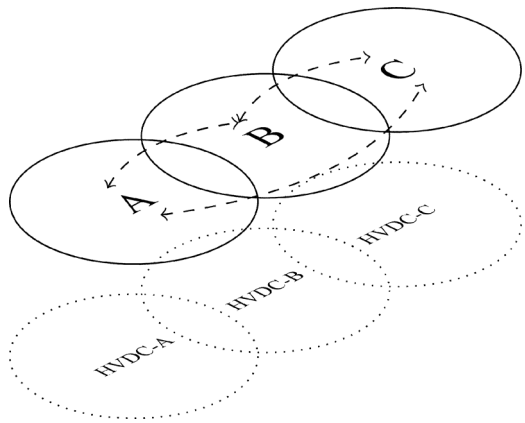

Fig. 3. Schematic depiction of operating scheme 3—"the HVDC-HVAC ISO".

TABLE I
Comparison of Operating Schemes—Operating Scheme 1 is the Full System ISO, Operating Scheme 2 is Separate HVAC and HVDC ISOs While Operating Scheme 3 is ISOs With Both HVAC and HVDC Portions

	Operating Scheme		
	1	2	3
solution			
central	✓		
distributed		✓	✓
technologies			
single (HVAC or HVDC)		✓	
multi (HVAC and HVDC)	✓		✓
system knowledge			
full	✓		
partial		✓	✓

of a new operating entity. The third proposal originates from the geographical splitting of the systems, with extensions into a second transmission technology being made by the respective ISO.

The centralized solution has the benefit of having complete knowledge of the system. The distributed solutions have the benefit of not changing the operating structure of the system, however the calculation framework is slightly modified. The distributed methods proposed in this paper replicate global observability by using repeated exchange of data and updated solutions.

In the following sections the problem formulations for the three different operating schemes will be presented. The problem formulation of the central ISO, operating scheme 1, will be used as a basis to present the basics. The problem formulations of operating schemes 2 and 3 will be used to describe the particularities introduced by the splitting of the grid operation into several entities to allow a distributed solution of the problem.

III. System Modeling

A. Linear System Model

For both the HVAC and HVDC systems a linear system approximation is used. This provides an acceptable trade-off between accuracy and computational time [12]. Using the linear formulation of the power flow equations, together with a quadratic cost function for the amount of power generated, the general OPF problem can be formulated as a quadratic-problem [13].

For the HVAC system, the active power flow F between nodes k and m is given by (1), assuming that the line is modeled as a series reactance X_{km}, with nodal voltage magnitudes U and nodal voltage angles θ. When per-unit voltage magnitudes, and small angle differences are considered, this can be approximated by (2) (see [14] for more details):

$$F_{km}^{AC} = \frac{\|U_k\|\|U_m\|}{X_{km}} \sin(\theta_k - \theta_m) \tag{1}$$

$$F_{km}^{AC} \approx \frac{\theta_k - \theta_m}{X_{km}}. \tag{2}$$

In the case of the HVDC grid, the full formulation for the power flow between nodes k and m is given by (3). Here the line is modeled as a series resistance R_{km}. With the assumption that the voltages only vary slightly from their nominal voltage, defined as 1 per unit, the approximation in (5) can be written:

$$F_{km}^{DC} = \frac{U_k \cdot (U_k - U_m)}{R_{km}} \tag{3}$$

$$u_k = U_k - U_{\text{ref}} \tag{4}$$

$$F_{km}^{DC} \approx \frac{(u_k - u_m)}{R_{km}}. \tag{5}$$

The voltages u_k and u_m in (5) are now defined as the deviation from a nominal voltage U_{ref} defined at a reference bus.

This formulation is based on the linearized HVDC power flow developed in [5]. This reference also contains a detailed comparison between a full OPF and the linearized approximation for a mixed HVAC-HVDC grid.

Using the linearized power flow equations, the power loss equations can be approximated as follows. The power losses P_{loss} of a line are quadratic in the current I flowing on the line, as given by (6). The amount of active power which is transported over a line is given by (7), where U_{nom} is the nominal system voltage. Using this relationship, (8) can be formulated. As such the power losses are approximately quadratic in the active power flow across the line, as given by (8). With the use of flat voltages the relationship is simplified further, as given by (9). The assumption that the losses can be represented by (9) can be taken further if it is assumed that all lines have similar impedance values. For the case of the considered test system, with a histogram of the line resistances given in Fig. 4, this assumption holds meaning that $P_{\text{loss}} \sim F_{km}^2$ can be used. However, the formulation is valid for $P_{\text{loss}} \sim RF_{km}^2$ as well. Other formulations in literature do not take losses into account at all, and while the simplification be a strong one, it ensures the convexity of the problem:

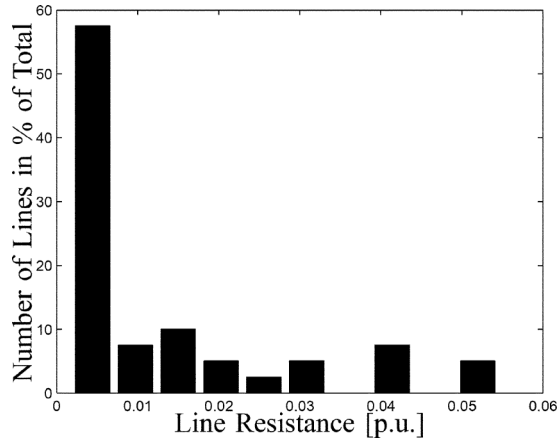

Fig. 4. Histogram of the per-unit line resistances for the RTS96 test system.

$$P_{\text{loss}} = I^2 R \tag{6}$$

$$F_{km} \approx U_{\text{nom}} I \tag{7}$$

$$P_{\text{loss}} \approx (\frac{F_{km}}{U_{\text{nom}}})^2 R \tag{8}$$

$$P_{\text{loss}} \sim RF_{km}^2. \tag{9}$$

In the formulation presented the losses in the terminals are not considered. While this does introduce some error, the main source of losses in the terminals are fairly constant, i.e., independent of loading, given as between 0.5% and 1.8% of the terminals nominal power by [15]. Reference [16] argues that approximately half of the losses in a HVDC terminal are constant losses, while the remaining half depends on the square of the current flowing through. When the voltage does not change abruptly, the square of the current and the power are linearly dependent, and the current-dependent losses could be approximated by a linear penalization of the power transferred by the terminal. The addition of such a loss term would be possible in all the three schemes proposed, and would not greatly influence the solution method.

B. Single Central Super-ISO

In the case of the single Super-ISO the problem to be solved is the selection of a cost-optimal generation and terminal exchange profile under consideration of the flows in the HVAC and HVDC lines. This can be formulated as an optimization problem.

1) Objective Function: The cost function for the optimization problem is given as in (10):

$$P_G^T \mathcal{C}^2 P_G + \mathcal{C}^1 P_G + \pi_{AC} \theta^T W_{rr}^{AC} \theta + \pi_{DC} U^T W_{rr}^{DC} U. \tag{10}$$

P_G is the vector of generation, $\mathcal{C}^2$ is the quadratic cost diagonal matrix for generation, and $\mathcal{C}^1$ is the linear cost vector for generation. θ is the vector of nodal voltage angle differences relative to the reference angle and U the nodal voltage differences in the HVDC grid relative to the reference bus. The formulation proposed here includes minimization of the generation costs as well as accounting for transmission losses. This represents maximizing social welfare. While it may not be in the direct interest

of the system operator to maximize social welfare, the authors believe that the regulator should give the operator the proper incentives so that demands of society are included in the objective of the operator. We assume that all operators have the same objectives, it would however be possible to use different cost functions for different operators, but the consideration of this is outside the scope of the paper.

Using the linear system formulation, the losses can be approximated without explicitly calculating them, as shown in (6)–(9). The matrices W_{rr}^{AC} and W_{rr}^{DC} are used to calculate the flows for HVAC and HVDC portions respectively, with these flows being penalized by π_{AC} and π_{DC}. It should be noted that the flows are not explicitly calculated, rather these terms are proxies for the physical losses.

2) Equality Constraints: The equality constraints for the optimization problem are given by

$$\Pi_G^{AC} P_G - \Pi_T^{AC} P_T - B^{AC}\theta - \Pi_L^{AC} L = 0 \quad (11)$$

$$\Pi_G^{DC} P_G + \Pi_T^{DC} P_T - B^{DC} U - \Pi_L^{DC} L = 0 \quad (12)$$

where Π_G^{AC} and Π_G^{DC} describes the incidence of generators to nodes in HVAC and HVDC grids respectively, while Π_T^{AC} and Π_T^{DC} describe the incidence of terminals to the HVAC and HVDC grids. P_T denotes the power flowing through a terminal, B^{AC} is bus susceptance matrix for the HVAC, while and B^{DC} is the bus conductance matrix for the HVDC grids. Π_L^{AC} and Π_L^{DC} are the load to node incidence matrices, and L is the vector of loads. For each node in the system, the amount of power generated minus the amount of power flowing out of the node, by terminal transfers, lines or load consumption, must be equal to zero. For each terminal the power being fed into it must be consumed at the other end. In the system considered here a positive flows direction for the terminals implies their use as load units in the HVAC system, but as generation units in the HVDC system. As the flow can be either negative or positive, the terminals can act as either load or generation units in both the HVAC and HVDC grids.

3) Inequality Constraints: The inequality constraints are given by

$$\underline{F}^{AC} \le F^{AC} \le \overline{F}^{AC} \quad (13)$$

$$\underline{F}^{DC} \le F^{DC} \le \overline{F}^{DC} \quad (14)$$

$$\underline{P_G} \le P_G \le \overline{P_G} \quad (15)$$

$$\underline{P_T} \le P_T \le \overline{P_T}. \quad (16)$$

The flows are given by $F^{AC} = B_f^{AC}\theta$ and $F^{DC} = B_f^{DC} U$, with $\underline{F}$ and $\overline{F}$ denoting minimum and maximum values. The same notation of minimum and maximum values is used for the generator and terminal injections. B_f is the line susceptance network matrix. B_f is of dimension $l \times n$, where l is the number of lines and n the number of buses.

IV. Distributed Calculation

The central solution to the power flow (PF), OPF, and SCOPF problems for HVAC grids have been considered in great detail in a large number of publications, with [17] providing a good overview.

The problem of distributed solution is not as well studied, but has been considered in a number of publications. Reference [18] is one of the earliest. A large body of work has been performed by the authors of [19]–[21]. A solid theoretical background, with the requirements for convergence can be found in [22] and [23]. Practical implementation of the problem has been considered by [24] and [25]. The use of decentral calculations to schedule FACTS devices is considered in [26].

In the following we will introduce the distributed formulation, and then describe its application to the operating schemes. The solution of the general OPF formulation in a distributed manner is solved using an iterative approach, as given by (17). This iterative approach uses both external and internal information, $\mathcal{X}_E$ and $\mathcal{X}_I$, respectively, to calculate a new update. As the aim is to reach an agreement between internal and external areas, the new update is given by minimizing a function $\mathcal{F}$ describing a deviation measure:

$$\min \mathcal{F}(\mathcal{X}_I^{(\kappa)}, \mathcal{X}_I^{(\kappa-1)}, \mathcal{X}_E^{(\kappa-1)}). \quad (17)$$

The updated value $\mathcal{X}_I^{(\kappa)}$ is generally a weighted average of the calculated update and the previous values, shown in (18). The damping factor γ is used to weight the answer from the previous iteration step in order to avoid oscillations in the results. Here $\hat{\mathcal{X}}_I^{(\kappa)}$ is the solution to (17), and $\mathcal{X}_I^{(\kappa)}$ is the value accepted as the current iteration step:

$$\mathcal{X}_I^{(\kappa)} = \gamma \mathcal{X}_I^{(\kappa-1)} + (1-\gamma)\hat{\mathcal{X}}_I^{(\kappa)}. \quad (18)$$

The detailed formulation of $\mathcal{F}$ is dependent on the problem to be solved. As in [7] a reduced distributed OPF formulation is used. In contrast to previous formulations, the border angles are not exchanged, the only agreement which must be reached is on the amount of power flowing across the border, and an explicit penalty is used for the border mismatch. The removal of border angle adherence allows us to have multiple reference buses in the interconnected system, one in each area, meaning that the selection of an area to contain the reference bus is no longer necessary. This formulation assumes that all operators have similar targets, the maximization of social welfare. Operators which have other targets are outside the scope of this paper, as the primary aim is on the description of the algorithm.

In the particular case of a simplified OPF problem, (17) can be formulated as in (19):

$$\min_{P_G, P_X, P_N} c_G(P_G^{\kappa}) + \alpha^{\kappa} P_X^{\kappa} + \pi_{\Delta} |P_X^{\kappa} - P_N^{\kappa}|. \quad (19)$$

Here P_G is the internal generation profile, P_X is the internal estimate of power exchanges, while P_N is the external estimate of power exchanges. $c_G(P_G)$ describes the cost of internal generation, given as a quadratic function of the generated amount, αP_X is the cost for power exchanges, and $\pi_{\Delta}|P_X - P_N|$ is a penalty term for the difference between internal and external estimates. In this formulation $\mathcal{X}_I = [P_G P_X]^T$ and $\mathcal{X}_E = P_N$. As such $\hat{\mathcal{X}}_I$ is the solution to (19). As the absolute term can not be implemented in a quadratic program, it is emulated by the square function. Meaning that $|P_X - P_N|$ is replaced by $(P_X - P_N)^2$. As P_N is not an optimization variable, this drives P_X towards P_N.

The inequality constraints of the optimization problem are given by the limits on generation, imports and line flows. The equality constraints are given by the nodal power balance equations.

The linear cost term α is the cost of importing power from the neighboring area. It is given by the Lagrangian multiplier λ, associated with the power equality constraint on the border nodes of the neighboring system. Due to the definition of positive flow direction, a sign-change must be performed, so that $\alpha = -\lambda$. The Lagrangian is not driven toward zero. The corresponding local Lagrangian is not available until after the optimization problem has been solved. As such the two values may vary. However, in the experience of the authors they do not diverge substantially in the latter steps of the convergence.

In (19) there are several variables which change with each iteration, for the sake of legibility, the iteration counter κ has been omitted from these variables in the remainder of the paper.

The calculations are aimed at being performed by separate ISOs. In order to replicate this behavior without the need for a communication network, the solution of the individual optimization problems was performed in parallel as three separate processes on a single computer, with a data exchange round after each iteration. The difficulties introduced by network communications, and their treatment, are outside the scope of this paper.

In the following two sections, the two distributed operating schemes will be presented in more detail.

A. Single HVDC ISO With Multiple HVAC ISOs

In the case of the HVDC ISO, the system is split both at the terminals and along the geographical borders in the HVAC system.

The terminals are modeled as generation units in both the HVAC and HVDC systems. These generation units can have positive or negative generation depending on the direction of power flow. In the case of the HVAC system the cross-border lines are modeled in the same manner as the terminals, and are not distinguishable. We do not consider which entity has physical control of the terminals. However, as the two parties involved are in agreement of which actions should be performed, the executing party does not have additional influence, and is thus not important.

1) Objective Function: In this case the objective function for the HVAC grids becomes

$$P_G^T \mathcal{C}^2 P_G + \mathcal{C}^1 P_G + \pi_{AC} \theta^T W_{rr} \theta + \alpha P_X + \\ + \pi_\Delta |P_X - P_N|. \tag{20}$$

The HVDC grid cost function becomes

$$P_G^T \mathcal{C}^2 P_G + \mathcal{C}^1 P_G + U^T W_{rr} U + \alpha P_X + \\ + \pi_\Delta |P_X - P_N|. \tag{21}$$

2) Equality Constraints: The equality constraint in the HVAC grid becomes

$$\Pi_G^{AC} P_G + \Pi_X^{AC} P_X - B^{AC} \theta - \Pi_L^{AC} L = 0. \tag{22}$$

The terminal transfer P_T is replaced by P_X as it acts as an import/export for all areas. Π_X describes the incidence of imports.

The corresponding HVDC equality constraint becomes

$$\Pi_G^{DC} P_G + \Pi_X^{DC} P_X - B^{DC} U - \Pi_L^{DC} L = 0. \tag{23}$$

In the case of the HVDC grids the imports are positive through the terminals. The case of HVDC grids split along geographic borders is not considered, as such only a single HVDC ISO is employed.

3) Inequality Constraints: For both the HVAC and HVDC the inequality constraints remain the same as in (13)–(16). Only the constraints on terminal flows P_T are replaced with constraints on exchanges P_X.

B. Multiple HVAC-HVDC ISOs

In the case of HVDC-HVAC ISOs the splitting is performed along the geographical borders, but not between technologies. From this perspective the modeling of terminals as importing nodes cannot be made. The formulation in this case is more complicated than in both the single ISO and the HVDC ISO case.

1) Objective Function: The objective function for each area can be written in the same manner as for the single ISO, and is given by

$$P_G^T \mathcal{C}^2 P_G + \mathcal{C}^1 P_G + \alpha P_X + \\ + \pi_{AC} \theta^T W_{rr}^{AC} \theta + \pi_{DC} U^T W_{rr}^{DC} U + \\ + \pi_\Delta |P_X - P_N|. \tag{24}$$

2) Equality Constraints: In the case of the equality constraints the terminal flows must be explicitly considered, as must the exchange flows. Here the exchange flows can be both HVAC or HVDC flows. The incidence matrices Π_X^{AC} and Π_X^{DC} describe the connection points of the exchanges into the HVAC and HVDC grids:

$$\Pi_G^{AC} P_G - \Pi_T^{AC} P_T + \\ - B^{AC} \theta - \Pi_L^{AC} L + \Pi_X^{AC} P_X = 0 \tag{25}$$

$$\Pi_G^{DC} P_G + \Pi_T^{DC} P_T + \\ - B^{DC} U - \Pi_L^{DC} L + \Pi_X^{DC} P_X = 0. \tag{26}$$

3) Inequality Constraints: The form of the inequality constraints does not change, and remains as in (13)–(16).

V. Case Studies

A. Description of Test System

The grid used in this case study is based on the publicly available IEEE Reliability Test System (96) (RTS96) test system [27]. An illustration of the grid is shown in Fig. 5. It consists of three similar areas with 24 HVAC buses each. In the basic case, the load in all areas is equal. Therefore it can not be expected that there will be substantial power flows across the interconnections. As this paper is primarily considering the case where there is an influence between the systems, substantial tie-line flows are desired. In order to achieve this, the loads in Area 2 were increased uniformly by 25%. This load level will be referred to as nominal load from now on. The HVDC portion of the test system used is defined as follows. The positions for the HVDC terminal stations have been selected manually and shown in Table II. Each area is equipped with two terminal stations, each at a strongly meshed bus. The capacity of each terminal is 500 MW. Two additional HVDC buses are added to the HVDC grid as HVDC-only buses between the terminals. The first of these buses, Bus 7, is in Area 1 and the second, Bus 8, in Area 2. These 8 terminal stations are connected to a multi-terminal HVDC system with 16 HVDC lines; see Table III. The capacity of each added HVDC lines is 300 MW. For this particular case, the HVDC grid does not have any generation or load connected to it. As such, the HVDC grid is a pure energy-transport grid.

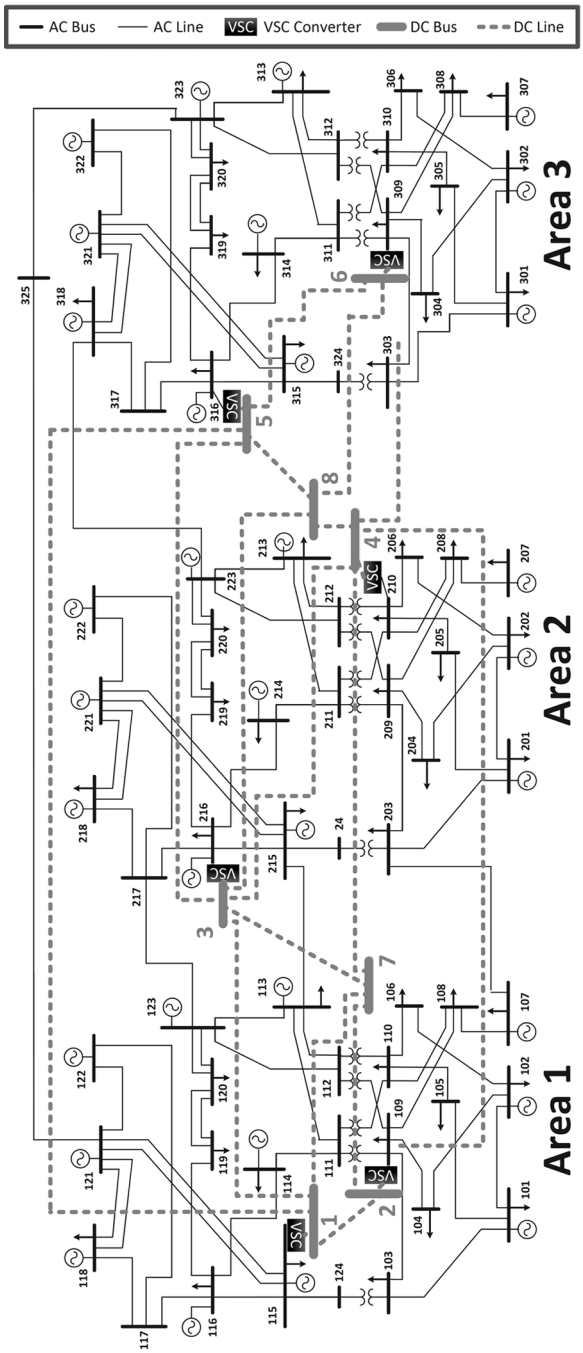

Fig. 5. Test system layout—3 interconnected 24-bus RTS systems with an overlay 8-bus HVDC grid.

TABLE II
POSITIONS OF THE HVDC TERMINALS, EACH WITH 500-MW CAPACITY

Terminal #	1	2	3	4	5	6	7	8
Connected to AC Bus #	115	109	216	210	316	309	No	No

B. Case Study Without HVDC

In order to show the functionality of the distributed formulation given in (19), the solution of the OPF problem in a pure HVAC grid is first considered as a base case. The solution obtained from the distributed method is compared to the solution received when using the software Matpower [28]. This section serves to verify the correctness of the simplified formulation.

TABLE III
POSITIONS OF GRID REINFORCEMENTS, EACH WITH 300-MW CAPACITY. BUS NUMBERS DENOTE BUSES IN THE HVDC GRID

Line #	1	2	3	4	5	6	7	8
From	1	1	1	1	2	2	3	3
To	2	3	5	7	4	7	4	5
Line #	9	10	11	12	13	14	15	16
From	3	3	4	4	4	5	5	6
To	7	8	6	7	8	6	8	8

TABLE IV
GENERATION COSTS FOR THE RTS96 TEST SYSTEM WITHOUT ADDITIONAL HVDC LINES. *NOTE*: THE ACTUAL RELATIVE DIFFERENCE $-9.43 \cdot 10^{-7}$ IS LOWER THAN THE SOLVER TOLERANCE

Solution Method	Total Generation Costs
Independent Verification	133734.55
Decentral Solution	133734.43
Relative Difference	~ 0

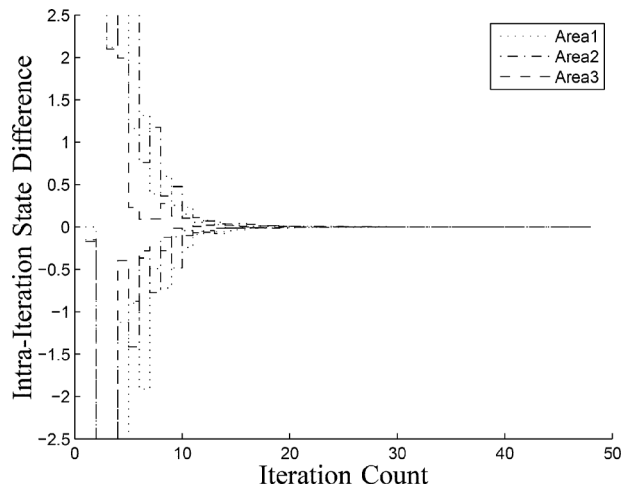

Fig. 6. Convergence of distributed approach on RTS96 without additional HVDC grid.

1) Operating Costs: The operating costs for the test system is shown in Table IV. It can be seen that the formulation for the distributed solution of the OPF problem formulated in this paper provides an almost identical solution. The comparison of the generation amount P_G for the centralized and decentralized cases is given by the relative difference of the generation profiles, and is given as $\epsilon_{rel} = (P_{G,d} - P_{G,c})/P_{G,c}$. The maximum 2-norm of ϵ_{rel} occurs in area 1, and is 0.0005, and the maximum ∞-norm of ϵ_{rel} is 0.0003, and also occurs in area 1. It should be noted that the difference arises due to the shift of generation between two generators with equal marginal cost.

2) Convergence: Fig. 6 shows the containing envelopes for the state-changes between two consecutive iterations, given as $\delta(\mathcal{X})^\kappa = \mathcal{X}^\kappa - \mathcal{X}^{(\kappa-1)}$. The envelope consists of the maximum and minimum values for each iteration step. This envelope reflects the convergence of the problem. In this particular case, the solution used a damping parameter, as shown in (18), of γ

TABLE V
COMPARISON OF THE NUMBER OF VARIABLES EXCHANGED FOR THE DISTRIBUTED SOLUTION WITHOUT HVDC GRID. A VARIABLE PAIR CONSISTS OF A NODAL PRICE λ AND A NODAL POWER INJECTION P_X

ISO	Variable Pairs	Partners
Area 1	4	2
Area 2	4	2
Area 3	2	2
Total	10	

TABLE VI
OPERATING COSTS UNDER DIFFERENT OPERATING SCHEMES—OPERATING SCHEME 1 IS THE "SUPER ISO", OPERATING SCHEME 2 CONTAINS SEPARATE HVAC AND HVDC ISOS, OPERATING SCHEME 3 HAS HVAC-HVDC ISOS. *NOTE*: THE ACTUAL DIFFERENCES FOR THE BASE CASE ($-3.45 \cdot 10^{-6}$ AND $-9.71 \cdot 10^{-7}$ ARE CLOSE TO, OR LOWER THAN, THE SOLVER TOLERANCE

Base Case - Nominal load		
	Absolute Cost	Relative Difference
Operating Scheme 1	133734.58	- NA -
Operating Scheme 2	133734.58	~ 0
Operating Scheme 3	133734.58	~ 0
Load Case 1 - High load in Area 1		
	Absolute Cost	Relative Difference
Operating Scheme 1	133197.02	- NA -
Operating Scheme 2	133200.54	$2.65 \cdot 10^{-5}$
Operating Scheme 3	133200.54	$2.65 \cdot 10^{-5}$
Load Case 2 - Low load in Area 2		
	Absolute Cost	Relative Difference
Operating Scheme 1	120880.04	- NA -
Operating Scheme 2	121219.85	$2.81 \cdot 10^{-3}$
Operating Scheme 3	121762.39	$7.30 \cdot 10^{-3}$

$= 0.1$ in order to be stable. The convergence of the method presented in this paper requires more iterations than those reported by [22], [25], however there are less variables exchanged. It is believed that the damping factor is responsible for the greater number of iterations required.

3) Data Exchange: The amount of data which has to be exchanged in this case is given by the number of interconnections, and is shown in Table V. Each variable pair consists of the amount of exchanged power P_X and the Lagrangian multiplier λ.

C. Case Study With HVDC

1) Operating Costs: The initial analysis between the three operating schemes and their solution is performed on the basis of system operating costs, in this case the cost of generation. The solutions are compared both on their absolute values, and on the relative differences. The relative difference is calculated using the solution under operating scheme 1 as the base value. The use of operating scheme 1 as a base case is due to it not being affected by the system splitting, this means that the problem is solved centrally. In this case only a single iteration is needed.

Table VI shows this comparison for three different system loadings: the base case, high load in area 1 with simultaneously low load in areas 2 and 3, and for low load in area 2 with nominal load in areas 1 and 3. In each case high load is given by a uniform increase of loading to 160% of nominal load, and the low load situation is characterized by a uniform reduction to 75% of nominal load.

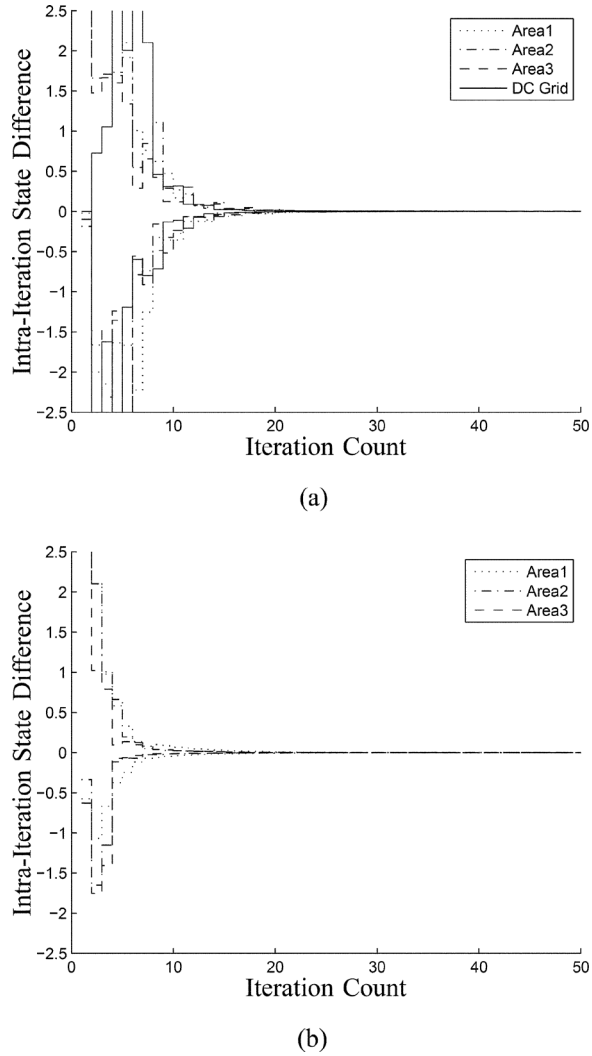

Fig. 7. Convergence of system state versus iterations. (a) State convergence of iterations for operating scheme 2. (b) State convergence of iterations for operating scheme 3.

As expected there is significant difference between the three load cases. However, there is little difference between the three operating schemes within a load case. In particular for the nominal load case, there is almost no difference. While a minor difference does arise, this is so small that is in the order of magnitude of the solver tolerance, as such its exactness must be questioned. In load case 2 the difference is slightly larger, but still small. In load case 3 there is a 0.5% difference between operating schemes 2 and 3, and a larger error relative to the nominal load case. This small difference between the operating schemes shows that the proposed algorithm is able to find a solution which has the same costs as the central solution. Here the base case is extremely close, while load cases 1 and 2 are more typical results.

As for the case-study without the HVDC system, the error is calculated as ϵ_{rel}. For the nominal load case, area 1 has a ∞-norm of 0.007. The error is again in the switching of generation between generators with equal marginal costs.

2) Convergence: Figs. 7(a) and 7(b) show the convergence of the states of the participating areas. In all cases the difference between two iteration steps approaches zero. As in the case without

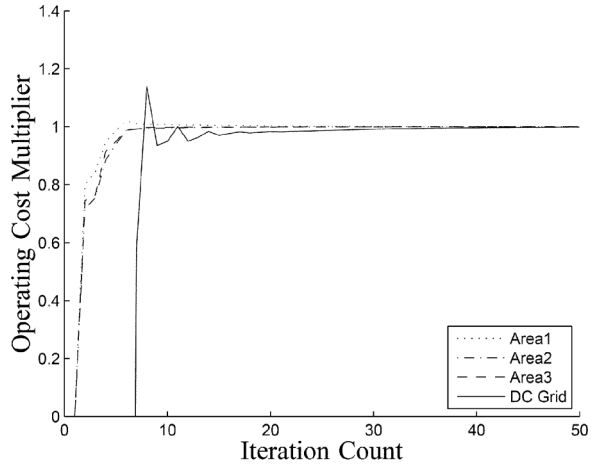

(a)

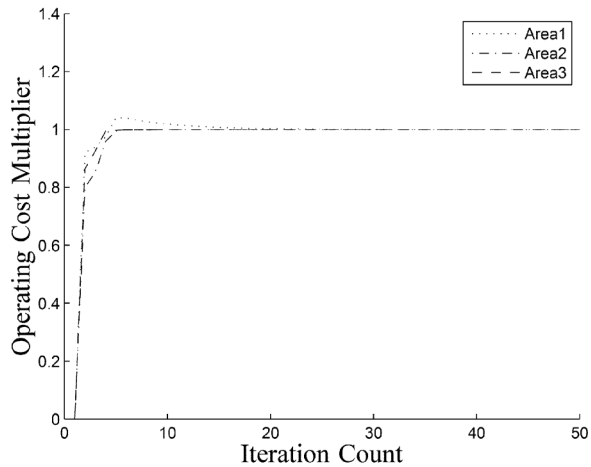

(b)

Fig. 8. Convergence of cost versus iterations. (a) Convergence of cost for operating scheme 2. (b) Convergence of cost for operating scheme 3.

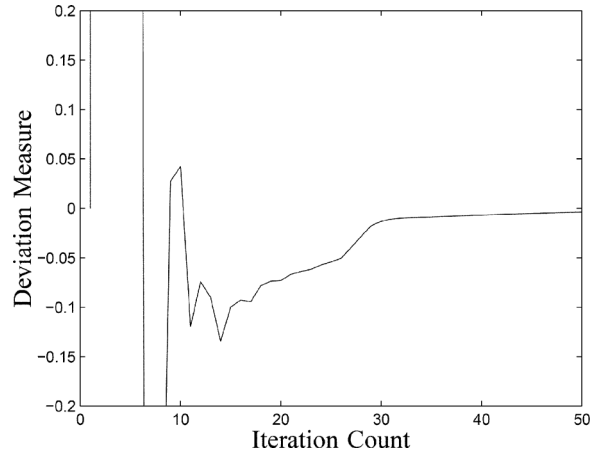

Fig. 9. Convergence of coupling variables in area 1 for operation scheme 2.

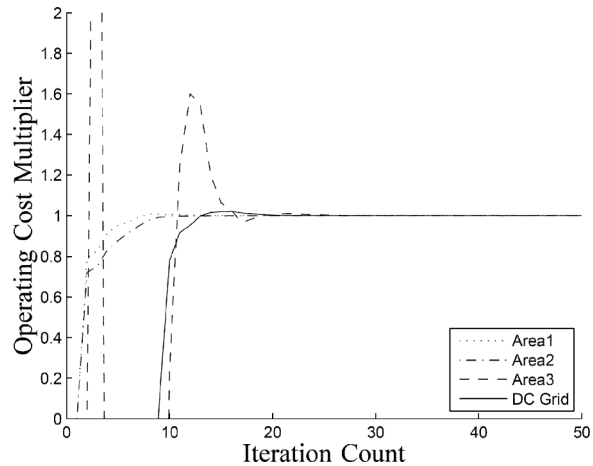

Fig. 10. Convergence of cost when area 3 is a transport grid. *Note: the image has been cropped to show the later convergence.*

a HVDC grid, the lines denote the envelope of changes in system state between two consecutive iterations. All system states, i.e., P_G, P_X, and the nodal voltage angles, are considered.

It can be seen that the convergence is faster in operating scheme 3. In this case sufficient convergence is achieved within 10 to 15 iterations. In operating scheme 2 this convergence requires between 20 and 25 iterations. In all cases the convergence values here were achieved with a damping factor $\gamma = 0.1$. This value was used to maintain comparability with the case study without the HVDC grid. In the test-system with HVDC grid, convergence can be achieved using $\gamma = 0$. This gives slightly less (by approximately 15%) iterations until convergence. The damping factor is empirically chosen, and is preferably small. For this particular case larger damping factors ($\gamma = 0.3, \gamma = 0.5$) do not greatly influence the number of iterations. The convergence of the cost, as shown in Fig. 8(a) and (b), shows similar behavior. For the sake of clarity, the costs are normalized to their final value. In the case of the operating scheme 3 convergence occurs by iteration 15, while under operating scheme 2 this process takes longer. It can clearly be seen that the HVDC ISO is the slowest to converge, with the HVAC areas requiring the same number of iterations before convergence in both cases. The penalty-term π_Δ is an empirical term, and the value selected for it greatly influences the convergence. It should be selected as large as possible, so that the values are driven towards each other quickly, but if it is too large convergence takes much longer. In the test $\pi_\Delta = 1$ was used. This gives a final value of $1.5 \cdot 10^{-12}$ for the deviation penalty, which compares to the total cost which is on the order of $1.5 \cdot 10^5$. Fig. 9 shows the evolution of the deviation on the border nodes for area 1 in the base case. The biggest single deviation is around $1 \cdot 10^{-6}$. The reason for the greater number of iterations in operating scheme 2 requires further examination. A reasonable explanation is that there is no generation capacity in the HVDC grid, meaning that it is totally dependent on the other grids. This statement is supported by the fact that the costs for the HVAC systems have stabilized before the cost for the HVDC system. This finding is supported by a test performed when the load in area 3 is reduced to zero, and the generation capacity removed. The cost convergence for this case is shown in Fig. 10, where it can clearly be seen that the two pure transport grids are the slowest to converge.

3) Data Exchange: Table VII shows the number of variables which are exchanged for each ISO and operating scheme. As the number of interconnections between the HVDC and HVAC grids is weaker than the interconnection within the HVDC grid, the number of variables used in operating scheme 3 is higher. On the other hand, the ISOs in this scheme have less partners to co-ordinate with.

TABLE VII
COMPARISON OF THE NUMBER OF VARIABLES EXCHANGED FOR THE DIFFERENT OPERATING SCHEMES. A VARIABLE PAIR CONSISTS OF A NODAL PRICE λ AND A NODAL POWER INJECTION P_X

ISO	Operating Scheme 2		Operating Scheme 3	
	Variable Pairs	Partners	Variable Pairs	Partners
Area 1	6	3	9	2
Area 2	6	3	12	2
Area 3	4	3	7	2
HVDC	6	3	- NA -	
Total	22		28	

VI. CLOSURE

A. Conclusions

This paper presents a distributed OPF formulation which can be used in cases where both HVAC and HVDC interconnections are used. Two different interconnection schemes are proposed and solved. The formulation presented is a reduced approach to the distributed OPF formulation, which requires less variables to be exchanged. While the amount of data exchanged is small, this reduction represents a saving of approximately 1/3 per variable pair. This could reduce both transmission cost and time, helping the ISOs.

This paper compares the performance of these interconnections relative to the solution provided by a central solution in terms of correctness and iteration count. Three different load situations are considered. In all considered cases, the solutions have high accuracy.

The method presented in this paper does not strive to find a faster solution, rather the explicit desire is to develop a method where the solution of the interconnected system does not rely on full system knowledge. Very limited knowledge about the external system is assumed: only the amount and price of power to be exchanged is considered. As such the solution presented in this paper is consistent with a market approach where participants place generation bids at known locations.

With the work presented in this paper a method with which new transmission technologies can be included in the current distributed operation scheme is presented. It presents an alternative to the establishment of a Super ISO with full system knowledge. This paper makes no recommendation on which operating scheme should be employed, as there are no gross differences between their solution from a technical or operational aspect. This choice thus becomes a political and regulatory one.

The method presented makes no inherent assumptions on how the different grids of the sub-ISO are modeled. As such the inclusion of other controllable devices, such as FACTS or phase shifters is not excluded. Models for such devices are available in literature, such as [29], which could be suitably adopted. If such devices are internal to the areas, it is not believed that they would greatly impact the number of iterations required until solution, however the local solution time may increase slightly.

B. Further Work and Outlook

The test system considered in this paper is one which is well known. The order of magnitude of the number of interconnections is rather small, but not orders of magnitude different from that which can be expected in reality. The number of interconnections in the European system is usually less than 10 interconnections per border. This indicates that this model can readily be applied to the full European model.

TABLE VIII
LIST OF VARIABLES USED

Variable	Explanation
$P.$	vector of powers
G	pertaining to generation
X	pertaining to exchange
N	pertaining to neighbor
T	pertaining to terminal
Π	nodal incidence matrix
U	voltage difference vector
θ	angle difference vector
B_f	network flow matrix
B	network susceptance matrix
$\mathcal{F}$	deviation measure
κ	iteration counter
$\mathcal{X}_I, \mathcal{X}_E$	internal and external states
λ	Locational Marginal Price
$c(\cdot)$	cost function
$\mathcal{C}_2$	quadratic cost matrix
$\mathcal{C}_1$	linear cost vector
W_{rr}	flow penalty matrix
$\pi.$	penalty coefficient
Δ	pertaining to generation
AC	pertaining to HVAC system
DC	pertaining to HVDC system
α	import cost
γ	damping factor

This paper does not consider the SCOPF formulation. As shown in [7] there is a substantial error introduced into the system by the lack of modeling of the external area. With the introduction of the controllability available thanks to the use of HVDC technology, it is very likely that a static preventive approach to security consideration, as currently done may no longer be suitable. This paper makes no consideration on the post-contingency operation of the system. The authors believe that the co-operative determination of the post-contingency operation could be performed in the same manner as the pre-contingency consideration. In this case the number of variables exchanged would increase greatly. In order for such a problem to remain feasible suitable techniques, such expert knowledge or computational ones, must be employed in order to reduce the number of contingencies considered. The reduction of the number of variables transmitted per iteration then becomes important as well.

In the formulation presented here, it was assumed that all participants are benevolent and interested in cooperation under the same target. The assessment of the influence of a party with additional interests, possibly contrary or malevolent, party participating may bring additional insight, but it is likely that a third-party arbitration system may prevent the need for such consideration by forcing all participants to be cooperative.

APPENDIX

A list of variables used is provided in Table VIII.

REFERENCES

[1] E. Tröster, R. Kuwahata, and T. Ackermann, European grid study 2030/2050, Tech. rep., energynautics, 2011.

[2] D. V. Hertem and M. Ghandhari, "Multi-terminal VSC HVDC for the European supergrid: Obstacles," *Renew. Sustain. Energy Rev.*, vol. 14, no. 9, pp. 3156–3163, 2010.

[3] J. Beerten, S. Cole, and R. Belmans, "A sequential AC/DC power flow algorithm for networks containing multi-terminal VSC HVDC systems," in *Proc. 2010 IEEE Power and Energy Soc. General Meeting*, Jul. 2010, pp. 1–7.

[4] M. Baradar and M. Ghandhari, "A multi-option unified power flow approach for hybrid AC/DC grids incorporating multi-terminal VSC-HVDC," *IEEE Trans. Power Syst.*, vol. 28, no. 3, pp. 2376–2383, Aug. 2013.

[5] R. Wiget and G. Andersson, "DC optimal power flow including HVDC grids," in *Proc. Elect. Power and Energy Conf. (EPEC)*, Halifax, NS, Canada, Aug. 2013.

[6] S. Chatzivasileiadis, T. Krause, and G. Andersson, "Security-constrained optimal power flow including post-contingency control of VSC-HVDC lines," in *Proc. XII SEPOPE*, Rio de Janeiro, Brazil, May 2012, pp. 1–12.

[7] M. Vrakopoulou, S. Chatzivasileiadis, E. Iggland, M. Imhof, T. Krause, O. Mäkelä, J. L. Mathieu, L. Roald, R. Wiget, and G. Andersson, "A unified analysis of security-constrained OPF formulations considering uncertainty, risk, and controllability in single and multi-area systems," in *Proc. IREP Symp.*, Rethymnon, Greece, Aug. 2013.

[8] S. Chatzivasileiadis and G. Andersson, "Security constrained OPF incorporating corrective control of HVDC by linear approximations," in *Proc. 18th Power Syst. Computation Conf.*, Wroclaw, Poland, 2014.

[9] R. Wiget, E. Iggland, and G. Andersson, "Security constrained optimal power flow for HVAC and HVDC grids," in *Proc. PSCC 2014*, 2014.

[10] A.-K. Marten and D. Westermann, "Schedule for converters of a meshed HVDC grid and a contingency schedule for adaption to unscheduled power flow changes," in *Proc. 2013 IEEE Power and Energy Soc. General Meeting (PES)*, Jul. 2013, pp. 1–5.

[11] J. Beerten and R. Belmans, "Analysis of power sharing and voltage deviations in droop-controlled DC grids," *IEEE Trans. Power Syst.*, vol. 28, no. 4, pp. 4588–4597, Nov. 2013.

[12] B. Stott, J. Jardim, and O. Alsac, "DC power flow revisited," *IEEE Trans. Power Syst.*, vol. 24, no. 3, pp. 1290–1300, Aug. 2009.

[13] J. Sun and L. S. Tesfatsion, "DC optimal power flow formulation and solution using QuadProg," *Econ. Dept., Iowa State Univ.*, vol. 6014, pp. 1–36, 2006.

[14] A. Wood and B. Wollenberg, *Power Generation, Operation and Control*. New York, NY, USA: Wiley, 1996.

[15] W. Feng, A. Tuan, L.B. Tjernberg, A. Mannikoff, and A. Bergman, "A new approach for benefit evaluation of multiterminal VSC-HVDC using a proposed mixed AC/DC optimal power flow," *IEEE Trans. Power Del.*, vol. 29, no. 1, pp. 432–443, Feb. 2014.

[16] G. Daelemans, K. Srivastava, M. Reza, S. Cole, and R. Belmans, "Minimization of steady-state losses in meshed networks using VSC HVDC," in *Proc. 2009 IEEE Power Energy Soc. General Meeting*, Jul. 2009, pp. 1–5.

[17] F. Capitanescu, J.L. Ramos, P. Panciatici, D. Kirschen, A. M. Marcolini, L. Pkatbrood, and L. Wehenkel, "State-of-the-art, challenges, and future trends in security constrained optimal power flow," *Electr. Power Syst. Res.*, vol. 81, no. 8, pp. 1731–1741, 2011.

[18] J. Wernerus and L. Soder, "Area price based multi-area economic dispatch with tie line losses and constraints," in *Proc. IEEE/KTH Stockholm Power Tech Conf.*, Stockholm, Sweden, 1995, pp. 710–15.

[19] B. Kim and R. Baldick, "Coarse-grained distributed optimal power flow," *IEEE Trans. Power Syst.*, vol. 12, no. 1, pp. 923–939, Feb. 1997.

[20] R. Baldick, B.H. Kim, C. Chase, and Y. Luo, "A fast distributed implementation of optimal power flow," *IEEE Trans. Power Syst.*, vol. 14, no. 3, pp. 858–864, Aug. 1999.

[21] B.H Kim and R. Baldick, "A comparison of distributed optimal power flow algorithms," *IEEE Trans. Power Syst.*, vol. 15, no. 2, pp. 599–604, May 2000.

[22] J.A. Aguado, V.H. Quintana, and A.J. Conejo, "Optimal power flows of interconnected power systems," in *Proc. 1999 IEEE Power Eng. Soc. Summer Meeting*, 1999, vol. 2, pp. 814–819.

[23] F.J Nogales, F.J Prieto, and A.J Conejo, "A decomposition methodology applied to the multi-area optimal power flow problem," *Ann. Oper. Res.*, vol. 120, no. 1–4, pp. 99–116, 2003.

[24] A.G Bakirtzis and P.N Biskas, "A decentralized solution to the DC-OPF of interconnected power systems," *IEEE Trans. Power Syst.*, vol. 18, no. 3, pp. 1007–1013, Aug. 2003.

[25] P.N Biskas and A.G Bakirtzis, "A decentralized solution to the security constrained DC-OPF problem of multi-area power systems," in *Proc. 2005 IEEE Russia Power Tech*, 2005, pp. 1–7.

[26] G. Hug-Glanzmann and G. Andersson, "Coordinated control of facts devices in power systems for security enhancement," in *Proc. 2007 iREP Symp. Bulk Power Syst. Dynamics and Control—VII. Revitalizing Oper. Rel.*, Aug. 2007, pp. 1–10.

[27] G. Clifford, "The IEEE reliability test system: 1996," in *IEEE Winter Power Meeting, Paper 96 WM 326–9 PWRS*, 1996.

[28] R.D Zimmerman, C.E Murillo-Sánchez, and R.J. Thomas, "MATPOWER: Steady-state operations, planning, and analysis tools for power systems research and education," *IEEE Trans. Power Syst.*, vol. 26, no. 1, pp. 12–19, Feb. 2011.

[29] M. Noroozian and G. Andersson, "Power flow control by use of controllable series components," *IEEE Trans. Power Del.*, vol. 8, no. 3, pp. 1420–1429, Jul. 1993.

Emil Iggland (M'14) received the B.Sc., M.Sc., and Dr.Sc. degrees from ETH Zürich, Switzerland, in 2008, 2009, and 2014, respectively.

His research interest include system security and the operation of multi-area power system.

Roger Wiget (S'11) was born in Lucerne, Switzerland. He received the B.Sc. degree in electrical engineering and the M.Sc. degree in energy science and technology from the ETH Zürich, Switzerland, in 2009 and 2011, respectively. He is currently pursuing the Ph.D. at ETH Zürich.

He joined the Power Systems Laboratory of ETH Zürich, Switzerland, in 2011. His research is dedicated to HVDC networks.

Spyridon (Spyros) Chatzivasileiadis (S'04–M'14) received the Diploma in electrical and computer engineering from the National Technical University of Athens (NTUA), Greece, in 2007 and the Ph.D. degree from ETH Zürich, Switzerland, in 2013.

He is a postdoc research fellow at Lawrence Berkeley National Laboratory (LBNL), Berkeley, CA, USA. At ETH, he developed methods to integrate High-Voltage DC lines (HVDC) in power system planning and operation. In March 2014, he joined the Grid Integration Group at LBNL, where he works on dc microgrids and co-simulation tools to integrate Demand Response.

Göran Andersson (M'86–SM'91–F'97) received the M.S. and Ph.D. degrees from the University of Lund, Sweden, in 1975 and 1980, respectively.

In 1980, he joined ASEA's, now ABB's, HVDC division in Ludvika, Sweden, and in 1986, he was appointed full professor in electric power systems at KTH (Royal Institute of Technology), Stockholm, Sweden. Since 2000, he has been a full professor in electric power systems at ETH Zürich (Swiss Federal Institute of Technology), where he also heads the powers system laboratory. His research interests include power systems dynamics and control, power markets, and future energy systems.

Prof. Andersson is fellow of the Royal Swedish Academy of Sciences, and of the Royal Swedish Academy of Engineering Sciences. He was the recipient of the IEEE PES Outstanding Power Educator Award 2007 and of the George Montefiore International Award 2010.